GEOLOGY FOR SOCIETY

SINCE 1858

GEOLOGICAL
SURVEY OF
NORWAY

· NGU ·

NGU REPORT
2021.019

Helicopter-borne magnetic,
electromagnetic and radiometric
geophysical survey in Mjøsa
Innlandet county: Revised Edition.

Erratum

Errors were found in the original report 2021.019 which has been corrected in the revised edition. The revised NGU report 2021.019 replaces the previous report with the same number, 2021.019.

Changes made to the revised report: NGU Report 2021.019
- Corrections to the radiometric data processing using adequate processing coefficients.
- Consequently, changed parameter tables and updated all maps.
- Revision of the descriptions of the data acquisition and processing.

NORGES GEOLOGISKE UNDERSØKELSE
- NGU -

REPORT

Report no.: 2021.019	ISSN: 0800-3416 (print) ISSN: 2387-3515 (online)	Grading: Open

Title: Helicopter-borne magnetic, electromagnetic and radiometric geophysical survey in Mjøsa area, Innlandet county: Revised Edition.

Authors: Frida Mathayo Mrope, Marie-Andree Dumais, Frode Ofstad and Ying Wang	Client: NGU

County: Innlandet	Municipality: Gjøvik and Vestre Toten

Map-sheet name (M=1:250.000) Hamar	Map-sheet no. and -name (M=1:50.000) Gjøvik 1816-1

Deposit name and grid-reference: WGS84 UTM32N 475000E, 6530000N	Number of pages: 35 Map enclosures:	Price (NOK):

Fieldwork carried out: **Aug-Sept 2020**	Date of report: **January 2023**	Project no.: 388900	Person responsible: *Marco Brönner*

Summary:

NGU conducted an airborne geophysical survey in Mjøsa, Innlandet county as part of NGU's general airborne mapping program in 2020.

This report describes and documents the acquisition, processing, and visualization of the acquired datasets and presents them in maps. The geophysical surveys consist of 2146 line-km data, covering an area of 458 km^2 flown from August 30th to September 07th, 2020.

The NGU modified Geotech Ltd. Hummingbird frequency domain EM system supplemented by an optically pumped Cesium magnetometer and the Radiation Solutions 1024 channels RSX-5 spectrometer mounted on a AS350-B3 helicopter was used for data acquisition.

The survey was flown with 200 meters line spacing, azimuth 90°. Average speed was 130 km/h, and average height clearance of the EM bird was 50 m and 80 m for the spectrometer.

Collected data were processed at NGU using Geosoft Oasis Montaj software. Raw total magnetic field data were corrected for diurnal variation and levelled using standard micro levelling algorithm. Radiometric data were processed using standard procedures recommended by International Atomic Energy Association (IAEA).

EM data were filtered and levelled using both automated and manual levelling procedures. Apparent resistivity was calculated from in-phase and quadrature data for three coplanar frequencies (880 Hz, 6.6 kHz and 34 kHz), and for two coaxial frequencies (980 Hz and 7 kHz) separately using a homogeneous half space model of 500 ohm-m.

All data were gridded using cell size of 50x50 meters. Magnetic and radiometric data is presented as 40% transparent grids with shaded relief on top of topographic maps. EM data is presented as 30% transparent grids on top of topographic maps.

Keywords:	**Airborne**	**Geophysics**
Magnetic	**Gamma-ray spectrometry**	**Radiometric**
Electromagnetic	**Technical report**	

CONTENTS

FIGURES

TABLES

1. INTRODUCTION

In 2020 NGU acquired airborne geophysical data from parts of Innlandet county. The surveyed area is situated between a fjord, Randsfjorden to the left and Mjøsa lake to the right. The helicopter survey reported herein amounts to 2146 line-km, or 458 km^2, with areas covered shown in Figure 1. The survey area is marked with a red border and was flown from 30th of August to 7th of September 2020.

Figure 1: Helicopter survey area in Gjøvik and Vestre Toten.

Table 1. Flight specifications

Survey Name	Surveyed lines (km)	Surveyed area (Km^2)	Line direction	Average flight speed (km/h)
Mjøsa2020	2146	458	90	130

The objective of the airborne geophysical survey was to obtain a dense high-resolution magnetic, electromagnetic and radiometric data over the survey area. This data is

required for the enhancement of a general understanding of the regional geology of the area, with adjoining areas covered by other airborne surveys in earlier years.

In this regard, the new data can be used to map contacts and structural features within the survey area. It also improves defining the potential of known zones of mineralization, their geological settings, and identifying new areas of interest, as the dataset fills a gap in the high-resolution geophysical surveys of the region.

The survey incorporated the use of a Hummingbird™ 5-frequency electromagnetic system supplemented by a high-sensitivity Cesium magnetometer, gamma-ray spectrometer, and radar altimeter. A GPS navigation computer system with flight path indicators ensured accurate positioning of the geophysical data with respect to the World Geodetic System 1984 geodetic datum (WGS-84).

2. SURVEY SPECIFICATIONS

2.1 Airborne Survey Parameters

NGU used a modified Hummingbird™ electromagnetic and magnetic helicopter survey system designed to obtain low level, slow speed, detailed airborne magnetic and electromagnetic data (Geotech 1997). The system was supplemented by 1024 channel gamma-ray spectrometer, installed under the belly of the helicopter, which was used to acquire the radiometric data and map ground concentrations of Uranium (U), Thorium (Th) and Potassium (K), and radiation Total Counts (Tc).

A Eurocopter AS350-B3 (LN-OSD) from helicopter company Pegasus Helicopter AS was used to tow the bird. The survey lines were spaced 200 meters apart and oriented at 90°. The magnetic and electromagnetic sensors are housed in a 7-meter-long bird, flown at an average of 50 m above the topographic surface.

Rugged terrain and abrupt changes in topography affected the aircraft pilot's ability to 'drape' the terrain, meaning the average instrumental height was sometimes higher than the standard survey instrumental height, which is defined as 30 meters plus a height of obstacles (trees, power lines etc.) for EM and magnetic sensors.

The ground speed of the aircraft varied from 101 – 158 km/h depending on topography, wind direction and its magnitude. On average the ground speed during measurements is calculated to 130 km/h. Magnetic data were recorded at 0.2 second intervals resulting in approximately 7.2 meters average point spacing.

EM data were recorded at 0.1 second intervals resulting in data with a sample increment of 3.6 meters along the ground in average. Spectrometry data were recorded every 1 second giving a point spacing of approximately 36 meters. The above parameters allow recognizing sufficient detail in the data to detect subtle anomalies that may represent mineralization and/or rocks of different lithological and petrophysical composition.

A base magnetometer to monitor diurnal variations in the magnetic field was located at the base on August 30th, 2020. The GEM GSM-19 station magnetometer data were recorded once every 3 seconds. The CPU clock of the base magnetometer and the helicopter magnetometer were both synchronized to UTC (Universal Time Coordinates) through the built-in GPS receiver to allow correction of diurnals.

Navigation system uses GPS/GLONASS satellite tracking systems to provide real-time WGS-84 coordinate locations for every second. The accuracy achieved with no differential corrections is reported to be ± 5 meters in the horizontal directions. The GPS receiver antenna was mounted internally inside the canopy of the helicopter.

For quality control, the electromagnetic, magnetic, and radiometric, altitude and navigation data were monitored on four separate windows in the operator's display during flight while they were recorded in three data ASCII streams to the PC hard disk drive. Spectrometry data were also recorded to an internal hard drive of the spectrometer. The data files were transferred to the field workstation via USB flash drive. The raw data files were backed up onto USB flash drive in the field.

2.2 Airborne Survey Instrumentation

Instrument specification is given in Table 2. Frequencies and coil configuration for the Hummingbird EM system is given in Table 3.

Table 2. Instrument Specifications

Instrument	Producer/Model	Accuracy / Sensitivity	Sampling frequency / interval
Magnetometer	Scintrex Cs-2	<2.5 nT throughout range / 0.0006 nT √Hz rms	5 Hz
Base magnetometer	GEM GSM-19	0.1 nT	3 s
Electromagnetic	Geotech Hummingbird	1 – 2 ppm	10 Hz
Gamma spectrometer	Radiation Solutions RSX-5	1024 ch's, 16 litres down, 4 litres up	1 Hz
Radar altimeter	Bendix/King KRA 10A	± 5 ft 40 – 500 feet ± 5 % 100 – 500 feet ± 7 % 500 – 2500 feet	1 Hz
Pressure/temperature	Honeywell PPT	± 0.03 % FS	1 Hz
Navigation	Topcon GPS-receiver	± 5 meters	1 Hz
Acquisition system	NGU custom software		

Figure 2: Hummingbird system in air

Table 3. Hummingbird EM system, frequency, and coil configurations

Coils	Frequency	Orientation	Separation
A	7701 Hz	Coaxial	6.30 m
B	6606 Hz	Coplanar	6.30 m
C	980 Hz	Coaxial	6.025 m
D	880 Hz	Coplanar	6.025 m
E	34133 Hz	Coplanar	4.90 m

2.3 Airborne Survey Logistics Summary

A summary of the survey specifications is shown in Table 4.

Table 4. Survey Specifications Summary

Parameter	Specifications
Traverse (survey) line spacing	200 meters
Traverse line direction	E-W (90º)
Nominal aircraft ground speed	101 - 158 km/h
Average aircraft ground speed	130 km/h
Average sensor terrain clearance Mag	50 meters
Average sensor terrain clearance Rad	80 meters
Sampling rates:	
Magnetometer	0.2 seconds
EM	0.1 seconds
Spectrometer, GPS, altimeter	1.0 second
Base Magnetometer	3.0 seconds

3. DATA PROCESSING AND PRESENTATION

The magnetic, radiometric, and electromagnetic data were processed at NGU by Frida Mathayo Mrope, Marie-Andrée Dumais and Frode Ofstad. Ying Wang and Frode Ofstad acquired the data. The ASCII data files were loaded into three separate Oasis Montaj databases. All three datasets were processed consequently according to processing flow charts shown in Appendix A1, A2 and A3.

3.1 Total Field Magnetic Data

At the first stage the raw magnetic data was visually inspected, and spikes were removed manually. Non-linear filter was also applied to airborne raw data to eliminate short-period spikes. Typically, several corrections must be applied to magnetic data before gridding - heading correction, lag correction and diurnal correction.

Diurnal Corrections

The temporal fluctuations in the magnetic field of the earth affect the total magnetic field readings recorded during the airborne survey. This is commonly referred to as the magnetic diurnal variation. These fluctuations can be effectively removed from the airborne magnetic dataset by using a stationary reference magnetometer that records the magnetic field of the earth simultaneously with the airborne sensor at given short time interval.

Diurnal variation channel was inspected for spikes, and spikes were removed manually if necessary. Magnetic diurnals that were recorded on the base station magnetometer were within the standard NGU specifications during the entire survey (Rønning 2013). Diurnal variations were measured with GEM GSM-19 magnetometer. The base station computer clock was continuously synchronized with GPS clock. The recorded data are merged with the airborne data and the diurnal correction is applied according to equation (1).

$$\boldsymbol{B}_{Tc} = \boldsymbol{B}_T + (\bar{B}_B - \boldsymbol{B}_B), \tag{1}$$

Where:

$\mathbf{B}_{Tc}$ = Corrected airborne total field readings

$\mathbf{B}_T$ = Airborne total field readings

$\bar{B}_B$ = Averaged atum base level

$\mathbf{B}_B$ = Base station readings

The average datum base level ($\bar{B}_B$) was found to be:
  - 51475 nT for flight line L1 flown on 30/08/2020,
  - 51400 nT for flight lines L4, L5 and L6 flown on 01-02/09/2020, and
  - 51409 nT for flight lines L2 and L3 flown on 31/08/2020, L7 flown on 01-02/09/2020 and L8 and L9 flown on 07/09/2020.

Corrections for Lag and heading

Neither a lag nor cloverleaf tests were performed before the survey. According to previous reports the lag between logged magnetic data and the corresponding navigational data was 1-2 fids. These values were observed to have negligible effect on the processed results. A heading error for a towed system is usually either very small or non-existent. No lag and heading corrections were applied.

Magnetic data processing, gridding, and presentation

The total field magnetic anomaly data ($\mathbf{B}_{TA}$) were calculated from the total field data ($\mathbf{B}_{Tc}$) after subtracting the International Geomagnetic Reference Field (IGRF) model for the surveyed area (equation 2).

$$\boldsymbol{B}_{TA} = \boldsymbol{B}_{Tc} - IGRF \qquad (2)$$

IGRF 2020 model was employed in these calculations to deduct the magnetic field resulting from the earth's core.

The total field anomaly data were split into lines and then were gridded using a minimum curvature method with a grid cell size of 50 meters. This cell size is exactly one quarter of the 200 meters average line spacing. To remove small line-to-line levelling errors that were detected on the gridded magnetic anomaly data, the Geosoft microlevelling technique was applied on the flight line based magnetic database. Then, the microlevelled channel was gridded using minimum curvature method with 50 meters grid cell size.

The processing steps of magnetic data presented so far, were performed on point basis. The following steps are performed on grid basis.

The horizontal and vertical gradient along with the tilt derivative of the total magnetic anomaly were calculated from the microlevelled total magnetic anomaly grid. The magnitude of the horizontal gradient (HG) was calculated according to equation (3).

$$HG = \sqrt{\left(\frac{\partial(B_{TA})}{\partial x}\right)^2 + \left(\frac{\partial(B_{TA})}{\partial y}\right)^2} \qquad (3)$$

Where: $\mathbf{B}_{TA}$ is the microlevelled total field anomaly. The vertical gradient (VG) was calculated by applying a vertical derivative convolution filter to the microlevelled $\mathbf{B}_{TA}$ field. The tilt derivative (TD) was calculated according to equation (4).

$$TD = tan^{-1}\left(\frac{VG}{HG}\right) \qquad (4)$$

The results are presented in a series of coloured shaded relief maps (1:150.000). The maps are:
   A. Total magnetic field anomaly
   B. Horizontal gradient of total magnetic anomaly
   C. Vertical gradient of total magnetic anomaly
   D. Tilt derivative (or Tilt angle) of the total magnetic anomaly

These maps are representative of the distribution of magnetization over the surveyed area. The list of the produced maps is shown in Table 6.

3.2 Electromagnetic Data

The EM system transmits five fixed frequencies and records in-phase and quadrature responses for each of the five transmitter-receiver coil sets of the EM system. The received signals are processed and used for computation of apparent resistivity.

In-phase (IP) and quadrature (Q) data were filtered with 10 fiducial non-linear filter to eliminate spherical spikes, which were represented as irregular noise of large amplitude in records and high frequency noise of bird electronics. Then, a 20-fiducial low-pass filter was applied to suppress instrumental and cultural noise. These filters were not able to suppress all the noise completely due to irregular nature of the noise; hence, noises were manually removed. Also, shifts of IP and Q records with amplitude of 5-10 ppm were observed in some flights. Shifts were edited manually where possible.

To remove the effects of instrument drift caused by gradual temperature variations in the transmitting and receiving circuits, background responses were recorded during each flight. To obtain a background level, the bird is raised to an altitude of at least 1000 ft above the topographic surface so that no electromagnetic responses from the ground are present in the recorded traces.

The EM traces observed at this altitude correspond to a background (zero) level of the system. If these background levels are recorded at 20-30 minutes interval, then the drift of the system (assumed to be linear) can be removed from the data by resetting these high-altitude responses to the initial zero level of the system and calculating a linear fit among them. The drift was removed on a flight-by-flight basis before any further processing was carried out. Geosoft HEM module was used for applying the drift correction. Residual instrumental drift, usually small, but non-linear, was manually removed on a line-to-line basis.

When levelling of the EM data was complete, apparent resistivity was calculated from in-phase and quadrature components using a homogeneous half space model of the earth (Geosoft HEM module) for 6606, 7001, 980, 880 and 34133 Hz. A threshold value of 3 ppm was set for inversion, with a starting value of 500 ohm-m.

Electromagnetic field decays rapidly with the distance (height of the sensors) – as z^{-2} – z^{-5} depending on the shape of the conductors and, at certain height, signals from the ground sources become comparable with instrumental noise. Levelling errors or precision of levelling can lead sometimes to appearance of artificial resistivity anomalies when data were collected at high instrumental altitude. Application of threshold value (3 ppm) allows excluding such data from an apparent resistivity calculation, though not completely. It is particularly noticeable in low frequencies datasets.

Resistivity data were visually inspected; artificial anomalies associated with high altitude measurements were manually removed. Data recorded at the height above 150 meters were considered as non-reliable and were removed. Power lines strongly affected low frequency data – 880 and 980 Hz and a coaxial frequency, 7001 Hz. The most prominent noise from power lines were filtered manually.

3.3 Radiometric data

Airborne gamma-ray spectrometry data was processed to calculate the abundance of potassium (K), thorium (eTh), and uranium (eU) in rocks and weathered materials from measured gamma-rays emitted due to the natural decay of unstable isotopes of these radioelements (e.g. ^{40}K, ^{238}U and ^{232}Th). The data processing steps were based on the IAEA recommended method for U, Th and K (International Atomic Energy Agency, 1991; 2003). A short description of the individual processing steps of the methodology as adopted by NGU is given below.

Energy windows
The Gamma-ray spectra were initially reduced into standard energy windows corresponding to the individual radio-nuclides K, U and Th. Figure 3 shows an example of a Gamma-ray spectrum and the corresponding energy windows and radioisotopes (with peak energy in MeV) responsible for the radiation.
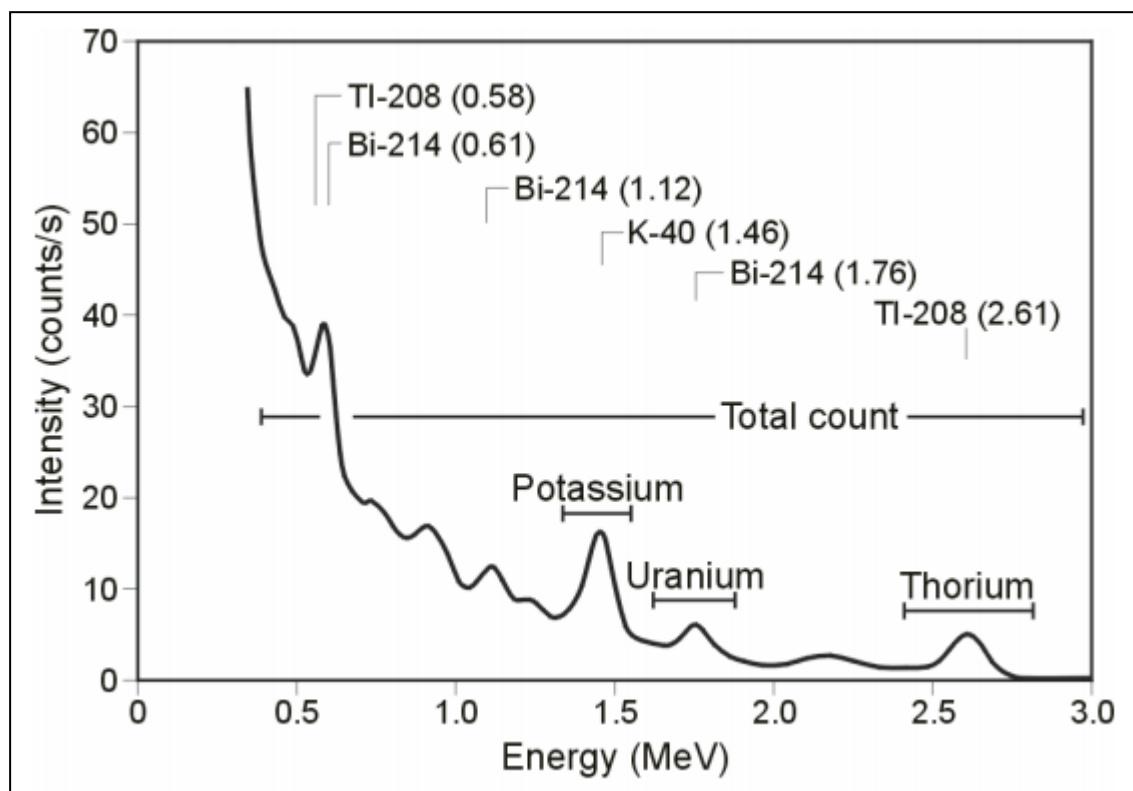

Figure 3: Gamma-ray spectrum with K, Th, U and Total Count windows.

Table 5. Specified windows for the 1024 RSX-5 system.

Gamma-ray spectrum	Cosmic	Total count	K	U	Th
Down	1023	137-937	457-523	553-620	803-937
Up	1023			553-620	
Energy windows (MeV)	>3.07	0.41-2.81	1.37-1.57	1.66-1.85	2.41-2.81

The RSX-5 is a 1024 channel system with four downward and one upward looking detector, which means that the actual Gamma-ray spectrum (0 -3 MeV) is divided into 1024 channels. The first channel is reserved for the "Live Time" and the last for the Cosmic rays. Table 5 shows the channels that were used to calculate window counts from the spectra.

Live Time correction
The data were corrected for live time. "Live time" is an expression of the relative length of time the instrument was able to register new pulses per sample interval. On the other hand, "dead time" is an expression of the relative length of time the system was unable to register new pulses per sample interval because it was busy in processing and registering of the incoming signals. The relation between "dead time" and "live time" is given by the equation (5)

$$\text{"Live time"} = \text{"Real time"} - \text{"Dead time"} \tag{5}$$

where the "real time" or "acquisition time" is the elapsed time over which the spectrum is accumulated (about 1 second).

The live time correction is applied to the total count, potassium, uranium, thorium, upward uranium, and cosmic windows. The formula used to apply the correction is as follows:

$$C_{LT} = C_{RAW} \cdot \frac{Acquisition\ Time}{Live\ Time} \tag{6}$$

where C_{LT} is the live time corrected window in counts per second, C_{RAW} is the raw window data in counts per second, while Acquisition Time and Live Time are in microseconds. In modern spectrometer like RSX-5, dead-time is only few microseconds.

Cosmic and aircraft correction
Background radiation resulting from cosmic rays and aircraft itself was removed from the total count, potassium, uranium, thorium, upward uranium windows using the following formula:

$$C_{CA} = C_{LT} - (a_c + b_c \cdot C_{Cos}) \tag{7}$$

where C_{CA} is the cosmic and aircraft corrected window, C_{LT} is the live time corrected window. a_c and b_c are aircraft background and cosmic coefficient for a particular window (i.e., K, U, Th and Total count). C_{Cos} is the low pass filtered cosmic window. a_c and b_c were calculated from a very high altitude (few thousand feet at a definite intervals) cosmic calibration flight.

Radon correction
The upward detector method, as discussed in IAEA (1991), was applied to remove the effects of the atmospheric radon in the air below and around the helicopter. Using window counts over water, where there is no contribution from the ground sources, enables the calculation of the coefficients (a_r and b_r) for the linear equations that relate the cosmic corrected counts per second of uranium window with that of total count, potassium, thorium, and upward uranium windows. Data over-land was used in conjunction with data over-water to calculate the a_1 and a_2 coefficients used in equation (8) for the determination of the radon component in the downward uranium window:

$$Radon_U = \frac{Uup_{CA} - a_1 \cdot U_{CA} - a_2 \cdot Th_{CA} + a_2 \cdot b_{Th} - b_U}{a_U - a_1 - a_2 \cdot a_{Th}} \qquad (8)$$

where $Radon_U$ is the radon component in the downward uranium window, Uup_{CA}, U_{CA} and Th_{CA} are upward uranium, downward uranium and thorium window counts after cosmic and aircraft background correction respectively. a_1, a_2, a_U, a_{Th}, b_U and b_{Th} are constants determined with suitable over-water and near-by over-land data (IAEA 1991).

The effects of radon in the downward uranium are removed by simply subtracting $Radon_U$ from U_{CA}. The effects of radon in the other windows are removed using the following formula:

$$C_{RC} = C_{CA} - (a_r \cdot Radon_U + b_r) \qquad (9)$$

where C_{RC} is the Radon corrected window, C_{CA} is the cosmic and aircraft corrected window, a_r is the proportionality factor and b_r is the constant determined from over-water data for K, Th and total count windows.

Compton Stripping
Radon corrected potassium, uranium and thorium windows are subjected to spectral overlap correction. Compton scattered gamma rays from higher energy isotope-decay (e.g. from pure Th source) are observed in lower energy windows of different radioelements (e.g. K and U) Similarly, high energy gamma-rays of ^{214}Bi from U decay series are also detected in Th window. Spectral overlaps were corrected by window stripping using stripping coefficients determined from measurements on calibrations pads (Grasty et al, 1991) at the Geological Survey of Norway in Trondheim (see values in Appendix A2).

The stripping corrections are given by the following formulas:

$$A_1 = 1 - (g \cdot \gamma) - (a \cdot \alpha) + (a \cdot g \cdot \beta) - (b \cdot \beta) + (b \cdot \alpha \cdot \gamma) \qquad (10)$$

$$U_{ST} = \frac{Th_{RC} \cdot ((g \cdot \beta) - \alpha) + U_{RC} \cdot (1 - b \cdot \beta) + K_{RC} \cdot ((b \cdot \alpha) - g)}{A_1} \qquad (11)$$

$$Th_{ST} = \frac{Th_{RC} \cdot (1 - (g \cdot \gamma)) + U_{RC} \cdot (b \cdot \gamma - a) + K_{RC} \cdot ((a \cdot g) - b)}{A_1} \qquad (12)$$

$$K_{ST} = \frac{Th_{RC} \cdot ((\alpha \cdot \gamma) - \beta) + U_{RC} \cdot ((a \cdot \beta) - \gamma) + K_{RC} \cdot (1 - (a \cdot \alpha))}{A_1} \qquad (13)$$

where U_{RC}, Th_{RC}, K_{RC} are the radon corrected uranium, thorium, and potassium respectively and a, b, g, α, β, γ are Compton stripping coefficients. U_{ST}, Th_{ST}, and K_{ST} are stripped windows of U, Th and K respectively.

Reduction to Standard Temperature and Pressure
The radar altimeter data were converted to effective height (H_{STP}) using the acquired temperature and pressure data, according to the expression:

$$H_{STP} = H \cdot \frac{273.15}{T + 273.15} \cdot \frac{P}{1013.25} \qquad (14)$$

where H is the smoothed observed radar altitude in meters, T is the measured air temperature in degrees Celsius and P is the measured barometric pressure in millibars.

Height correction

Variations caused by changes in the aircraft altitude relative to the ground was corrected to a nominal height of 60 m, the target height of the survey. Height attenuation factors are derived from special calibration flights at various intervals of altitudes between 100-600 feet over water and land spectrometry data.

Data recorded at the height above 150 m were considered as non-reliable and removed from processing. Total count, uranium, thorium, and potassium stripped windows were subjected to height correction according to the equation:

$$C_{60m} = C_{ST} \cdot e^{C_{ht} \cdot (60 - H_{STP})} \tag{15}$$

where C_{ST} is the stripped window, C_{ht} is the height attenuation factor for that window and H_{STP} is the effective (STP) height.

Conversion to ground concentrations

Finally, corrected count rates were converted to effective ground concentrations using calibration values (i.e sensitivity coefficients) derived from calibration pads (Grasty et al, 1991) at the Geological Survey of Norway in Trondheim (see values in Appendix A2). The corrected data provided an estimate of the surface concentrations of potassium, uranium, and thorium (K, eU and eTh). Potassium concentration is expressed as a percentage while equivalent uranium and thorium are calculated as parts per million (ppm). Uranium and thorium are described as "equivalent" since their presence is inferred from gamma-ray radiation of daughter elements (^{214}Bi for uranium, ^{208}Tl for thorium). The concentration of the elements is calculated according to the following expressions:

$$C_{CONC} = C_{60m}/C_{SENS\_60m} \tag{16}$$

where C_{60m} is the height corrected window counts, C_{SENS_60m} is sensitivity coefficient calculated to the nominal height (60m) using height attenuation coefficients.

Spectrometry data gridding and presentation

Gamma-rays from potassium, thorium and uranium emanate from the uppermost 30 to 40 centimetres of soil and bedrock (Minty, 1997). Variations in the concentrations of these radioactive elements are largely related to changes in the mineralogy and geochemistry of the Earth's surface.

The spectrometry data were stored in a database and the ground concentrations were calculated following the processing steps as described above. A list of the parameters used in these steps is given in Appendix A3.

The ground concentrations of the three main natural radio-elements potassium, thorium and uranium and total count were gridded using a minimum curvature method with a grid cell size of 50 meters.

Quality of the radiometric data was within standard NGU specifications (Rønning 2013). For further reading regarding standard processing of airborne radiometric data, we recommend the publications from Minty et al. (1997), IAEA (1991; 2003).

A list of the produced maps is shown in Table 6.

4. PRODUCTS

Processed digital data from the survey are presented as:
1. Geosoft XYZ files:
    Mjøsa_2020_Mag.xyz,
    Mjøsa_2020_EM.xyz,
    Mjøsa_2020_Rad.xyz

2. Grid-files in Geotiff format

Coloured maps at the scale 1:150 000 available from NGU on request.

Table 6. Maps available from NGU on request.

Map #	Name
2021.019-00	Survey Flight Path
2021.019-01	Total magnetic field
2021.019-02	Magnetic Horizontal Gradient
2021.019-03	Magnetic Vertical Gradient
2021.019-04	Magnetic Tilt Derivative
2021.019-05	Apparent resistivity, Frequency 7001 Hz, coaxial coils
2021.019-06	Apparent resistivity, Frequency 6606 Hz, coplanar coils
2021.019-07	Apparent resistivity, Frequency 980 Hz, coaxial coils
2021.019-08	Apparent resistivity, Frequency 880 Hz, coplanar coils
2021.019-09	Apparent resistivity, Frequency 34133 Hz, coplanar coils
2021.019-10	Radiometric Total counts
2021.019-11	Potassium ground concentration
2021.019-12	Uranium ground concentration
2021.019-13	Thorium ground concentration
2021.019-14	Radiometric Ternary Map

Downscaled images of the maps are shown on figures 4 to 18. Maps are presented with a scale of 1:150 000.

5. REFERENCES

IAEA 1991: Airborne Gamma-Ray Spectrometry Surveying, Technical Report No 323, Vienna, Austria, 97 pp

Geotech 1997: Hummingbird Electromagnetic System. User manual. Geotech Ltd. October 1997

Grasty, R.L., Holman, P.B. & Blanchard 1991: Transportable Calibration pads for ground and airborne Gamma-ray Spectrometers. Geological Survey of Canada. Paper 90-23. 62 pp.

IAEA 2003: Guidelines for radioelement mapping using gamma ray spectrometry data. IAEA-TECDOC-1363, Vienna, Austria. 173 pp.

Minty, B.R.S., Luyendyk, A.P.J. and Brodie, R.C. 1997: Calibration and data processing for gamma-ray spectrometry. AGSO – Journal of Australian Geology & Geophysics. 17(2). 51-62.

Naudy, H. and Dreyer, H. 1968: Non-linear filtering applied to aeromagnetic profiles. Geophysical Prospecting. 16(2). 171-178.

Rønning, J.S. 2013: NGUs helikoptermålinger. Plan for sikring og kontroll av datakvalitet. NGU Intern rapport 2013.001, (38 sider).

Appendix A1: Flow chart of magnetic processing

Processing flow:

- Quality control.
- Visual inspection of airborne data and manual spike removal
- Import of diurnal data.
- Correction of data for diurnal variation
- IGRF removed.
- Splitting flight data by lines
- Gridding

- Microlevelling using Geosoft menu.

Microlevelling parameters	Value
De-corrugation cutoff wavelength (m)	800
Cell size for gridding (m)	50
Amplitude limit (nT)	5
Naudy (1968) Filter length (m)	1000

Appendix A2: Flow chart of EM processing

Processing flow:
- Automated levelling using Geosoft HEM module.
- Filtering of in-phase and quadrature channels with non-linear and low-pass filters
- Quality control and visual inspection of data
- Manual removal of remaining part of instrumental drift
- Calculation of an apparent resistivity using in-phase and quadrature channels
- Splitting flight data by lines
- Gridding

Appendix A3: Flow chart of radiometry processing

Underlined processing stages are applied to the K, U, Th and total count windows.

- Airborne and cosmic correction (IAEA, 2003)
  Used parameters: determined by high altitude calibration flights (1500-9000 ft) at Langøya in 2013.

Channel	Background	Cosmic
K	8	0.0575
U	1	0.0471
Th	0	0.0638
Uup	0.3926	0.0107
Total counts	37	1.0263

- Radon correction using upward detector method (IAEA, 2003)
  Used parameters determined from survey data over water and land at Mjosa, August 2020.

Coefficient	Value	Coefficient	Value
a_u	0.1272	b_u	0.54662
a_K	2.97272	b_K	0.0
a_{Th}	0.09648	b_{Th}	1.1923
a_{TC}	28.92582	b_{TC}	5.35244
a_1	0.05695761	a_2	0.01543137

- Stripping corrections (IAEA, 2003)
  Used parameters determined from measurements on calibrations pads at NGU, May 2020.

Coefficient	Value
a	0.0469
b	0
c	0
α	0.3038
β	0.4685
γ	0.7964

- Height correction to a height of 60 m
  Parameters determined by high altitude calibration flights (100 – 700 ft). The average values from tests performed at Beitostølen, 2015 were used. Attenuation factors in 1/m.

Channel	Attenuation factor
K	-0.010179
U	-0.008477
Th	-0.008301
TC	-0.009447

- Converting counts at 60 m heights to element concentration on the ground
  Used parameters determined from measurements on calibrations pads at NGU, May 2020.

Channel	Sensitivity
K (%/count)	0.00764
U (ppm/count)	0.08849
Th (ppm/count)	0.15301
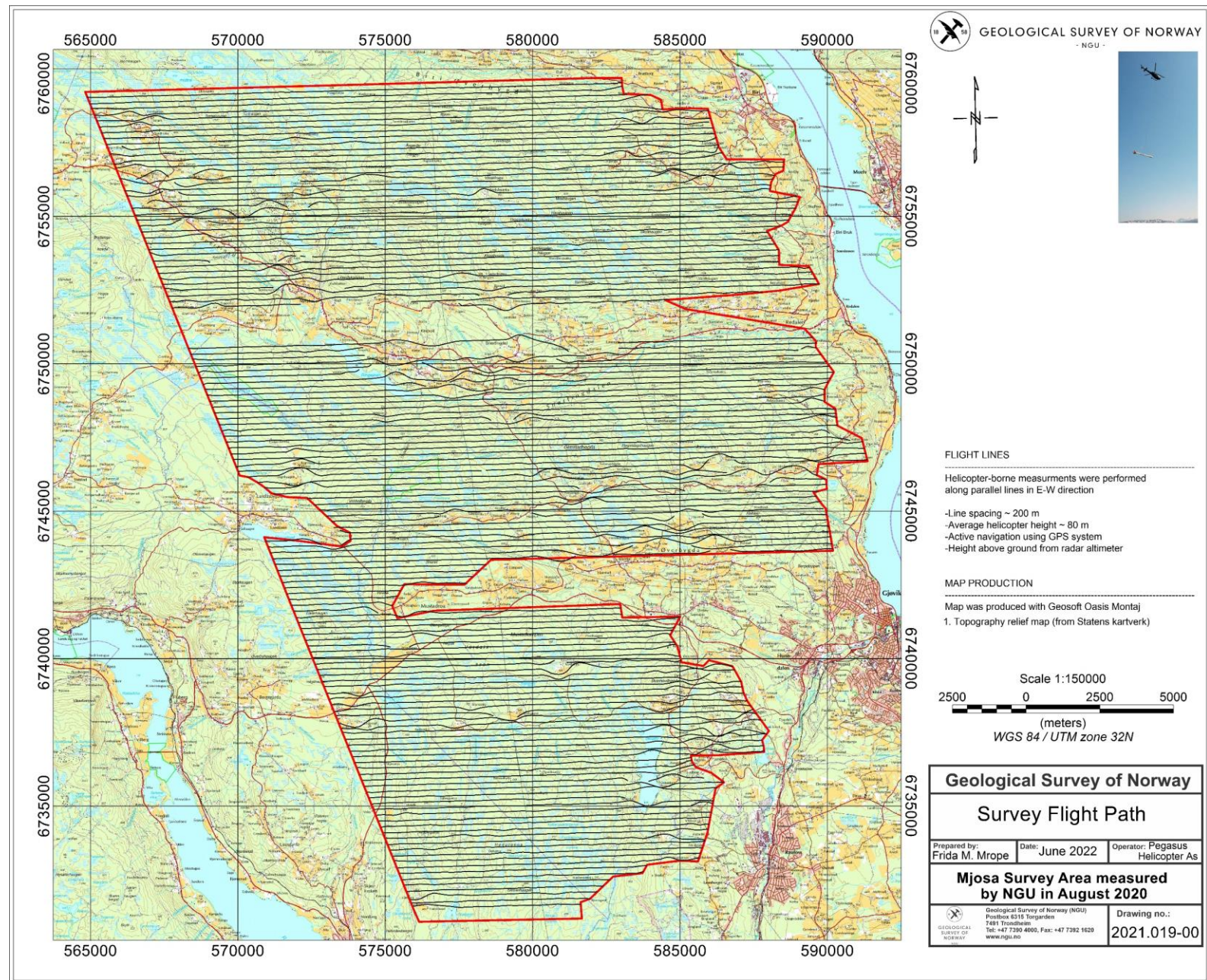
Figure 4: Mjøsa survey area with flight path.
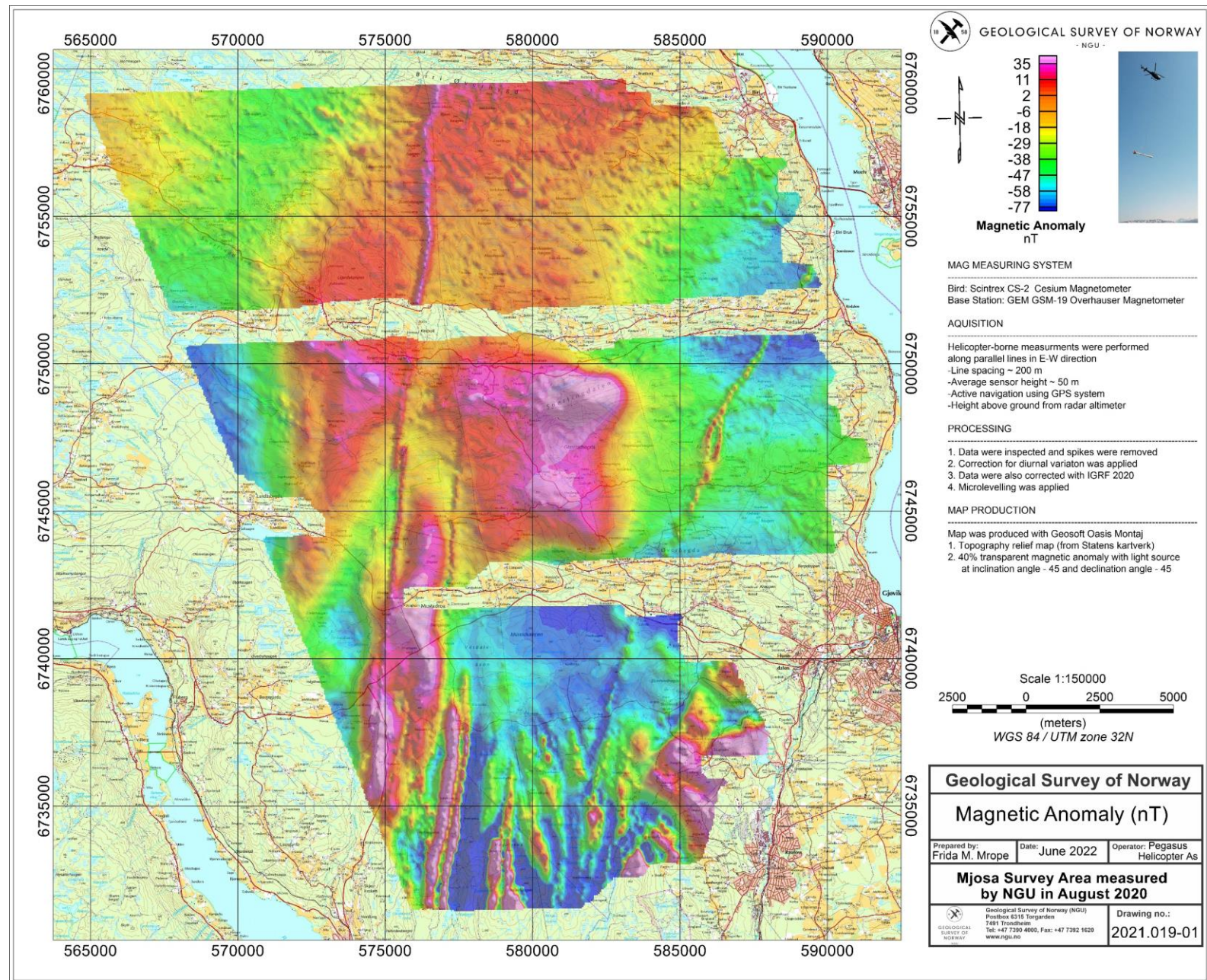
Figure 5: Total Magnetic Field.
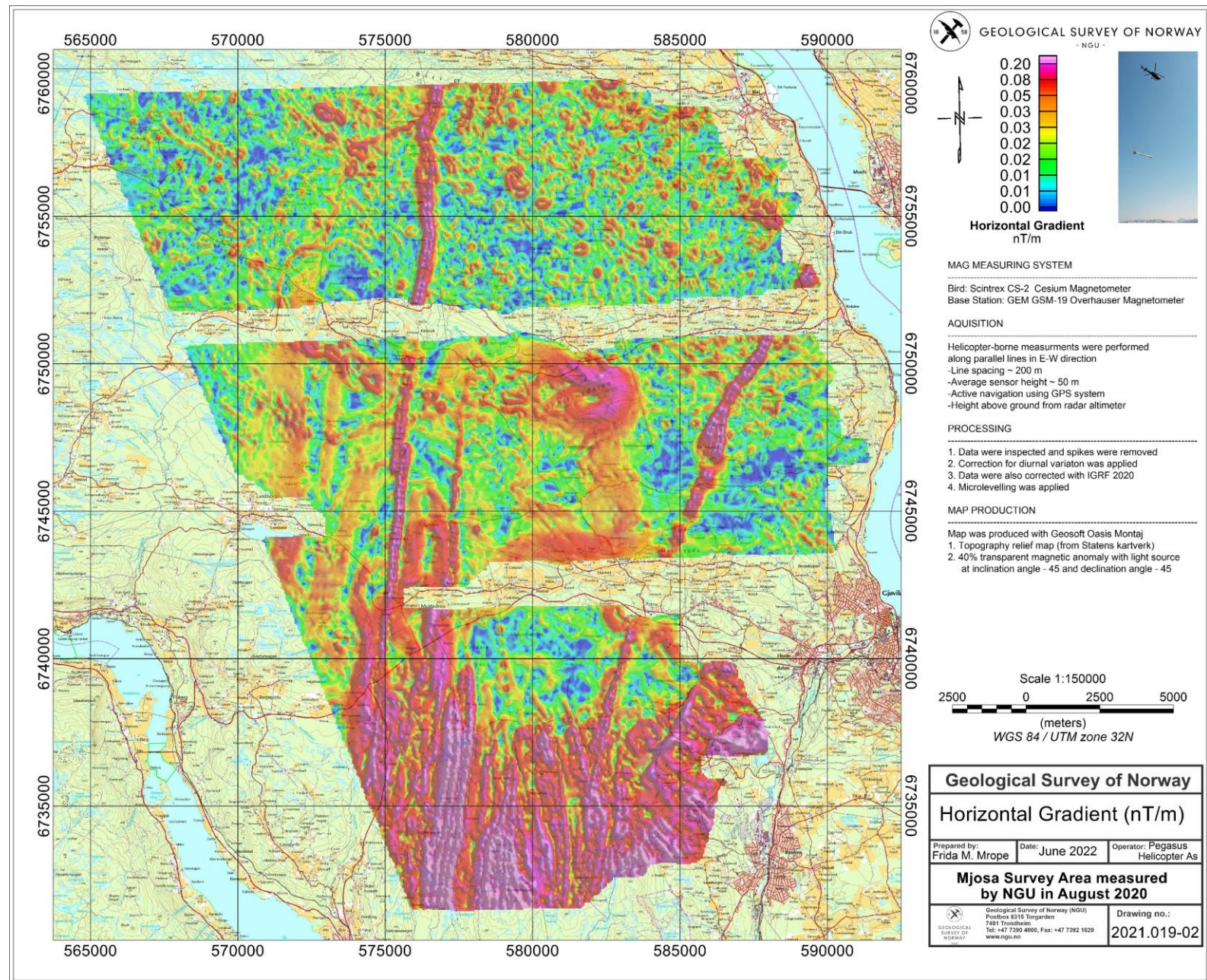
Figure 6: Magnetic Horizontal Gradient.

23
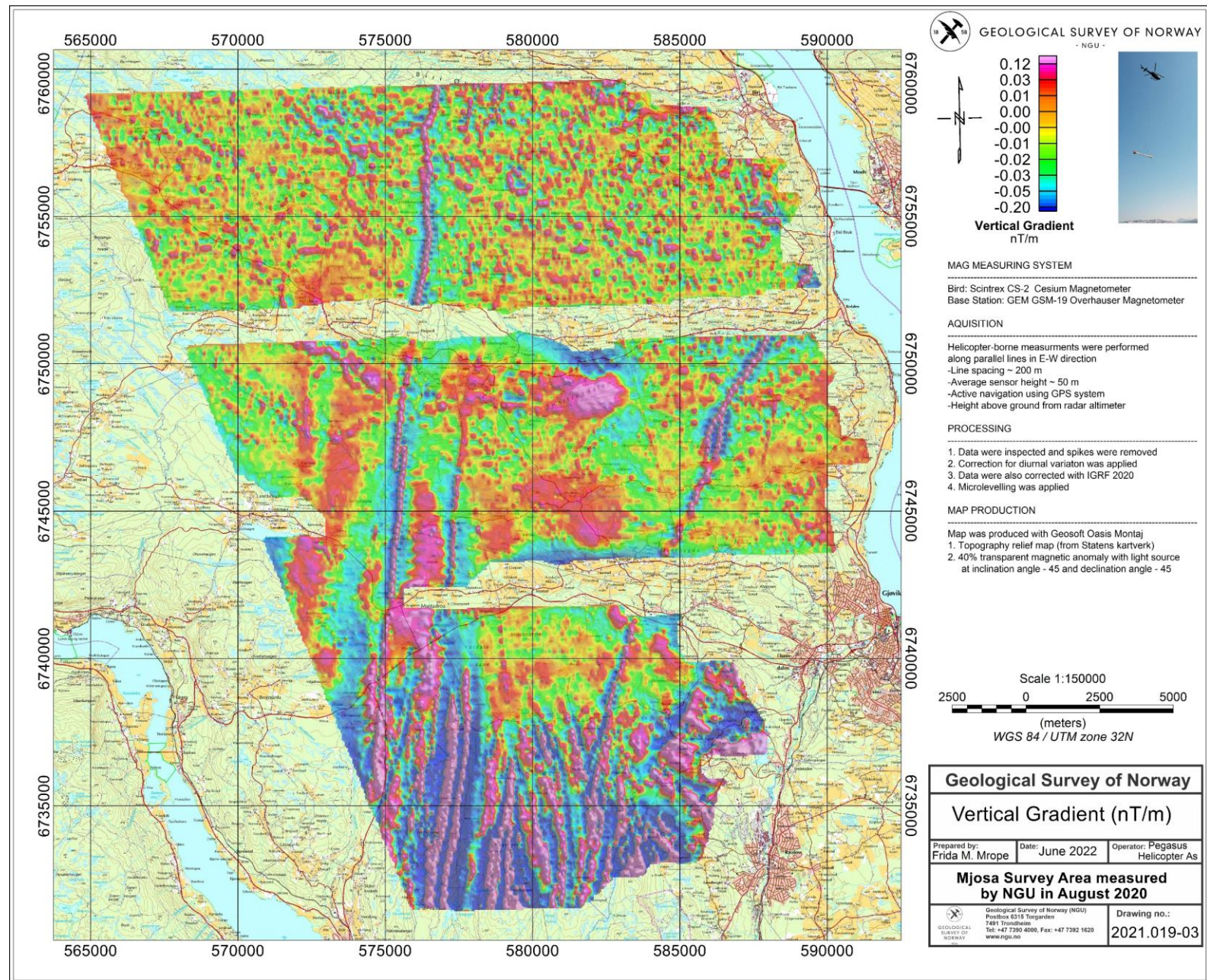
Figure 7: Magnetic Vertical Derivative.
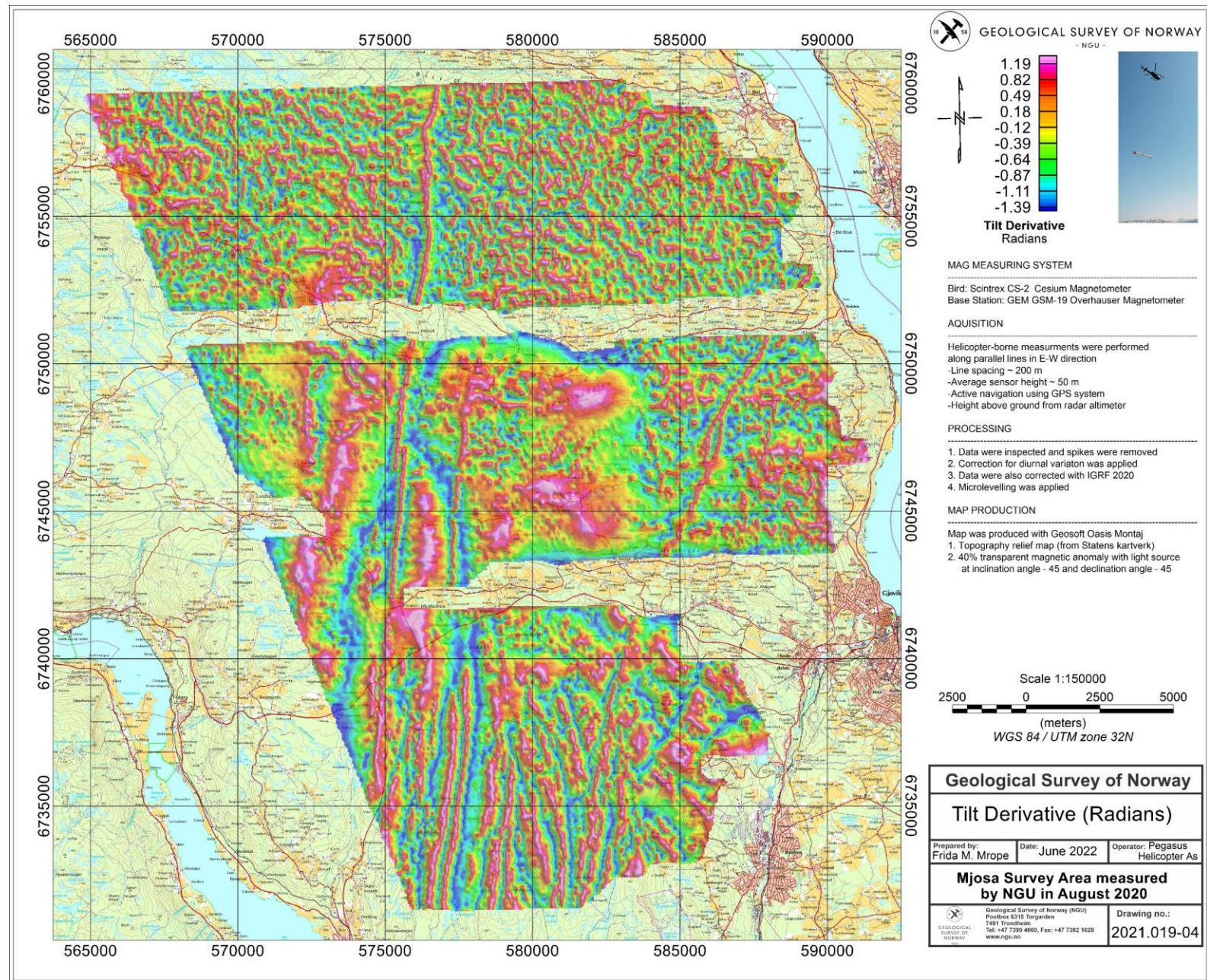
Figure 8: Magnetic Tilt Derivative.
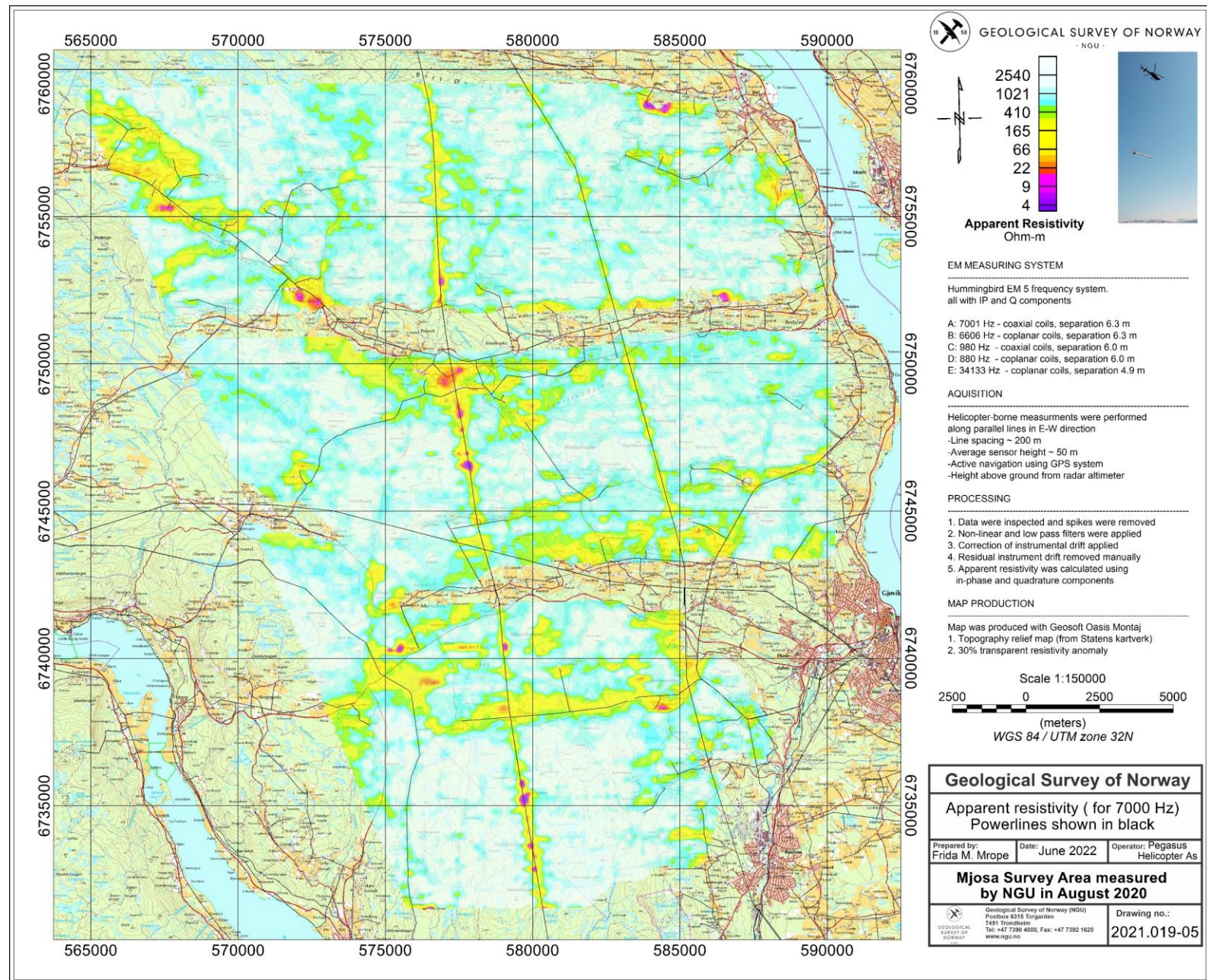
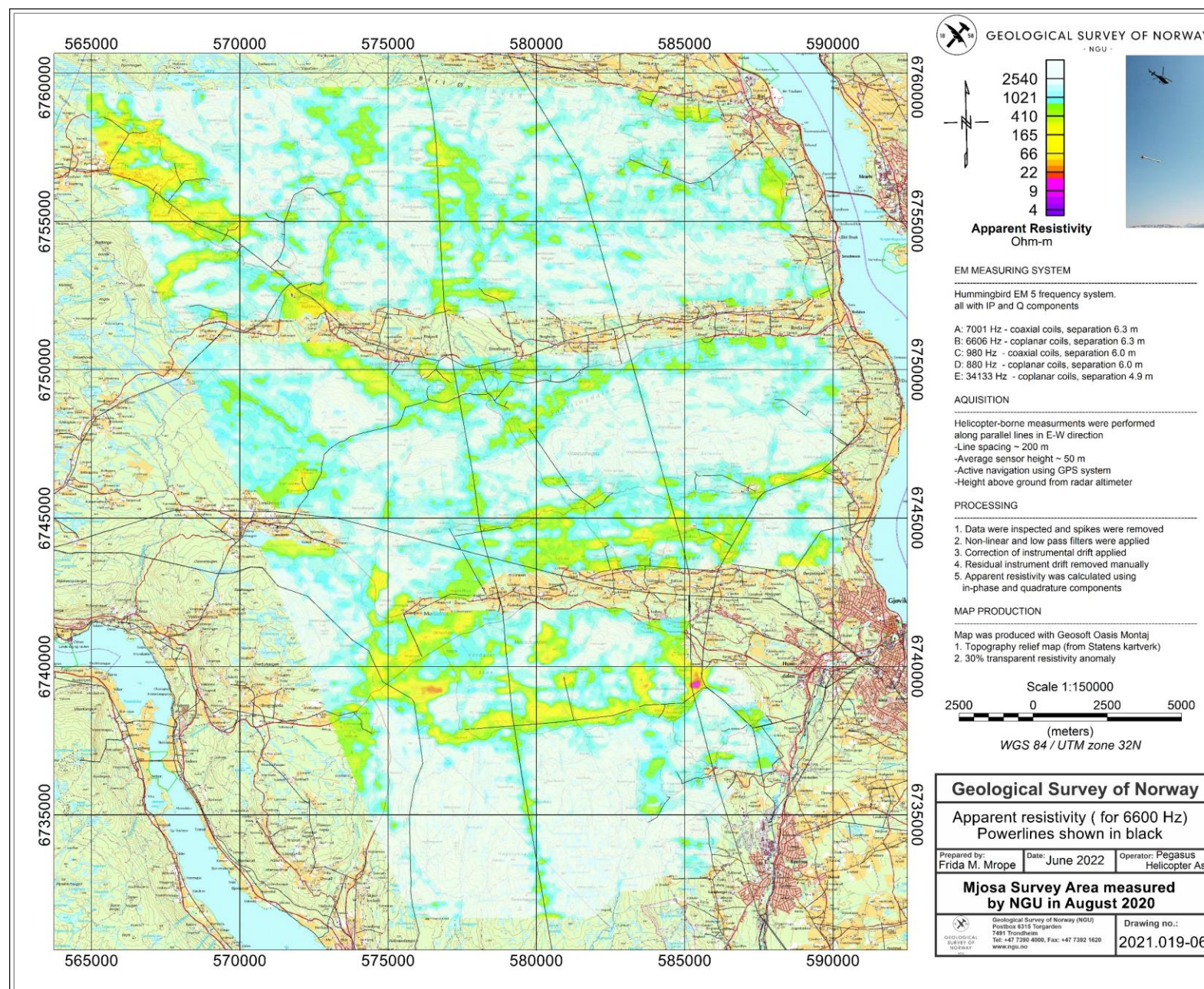**Figure 9: Apparent resistivity. Frequency 7001 Hz, Coaxial coils.**

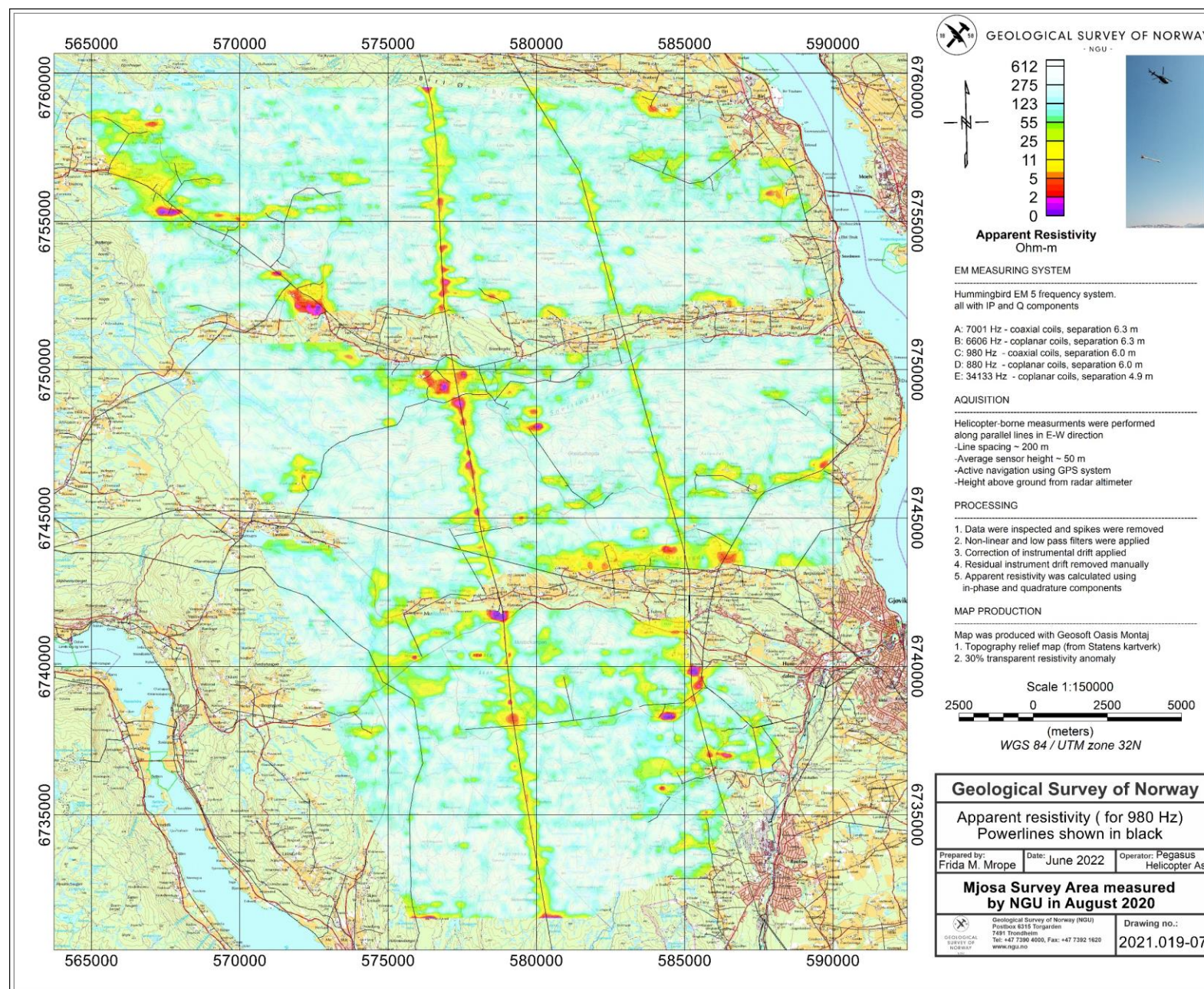**Figure 10: Apparent resistivity. Frequency 6606 Hz, Coplanar coils.**

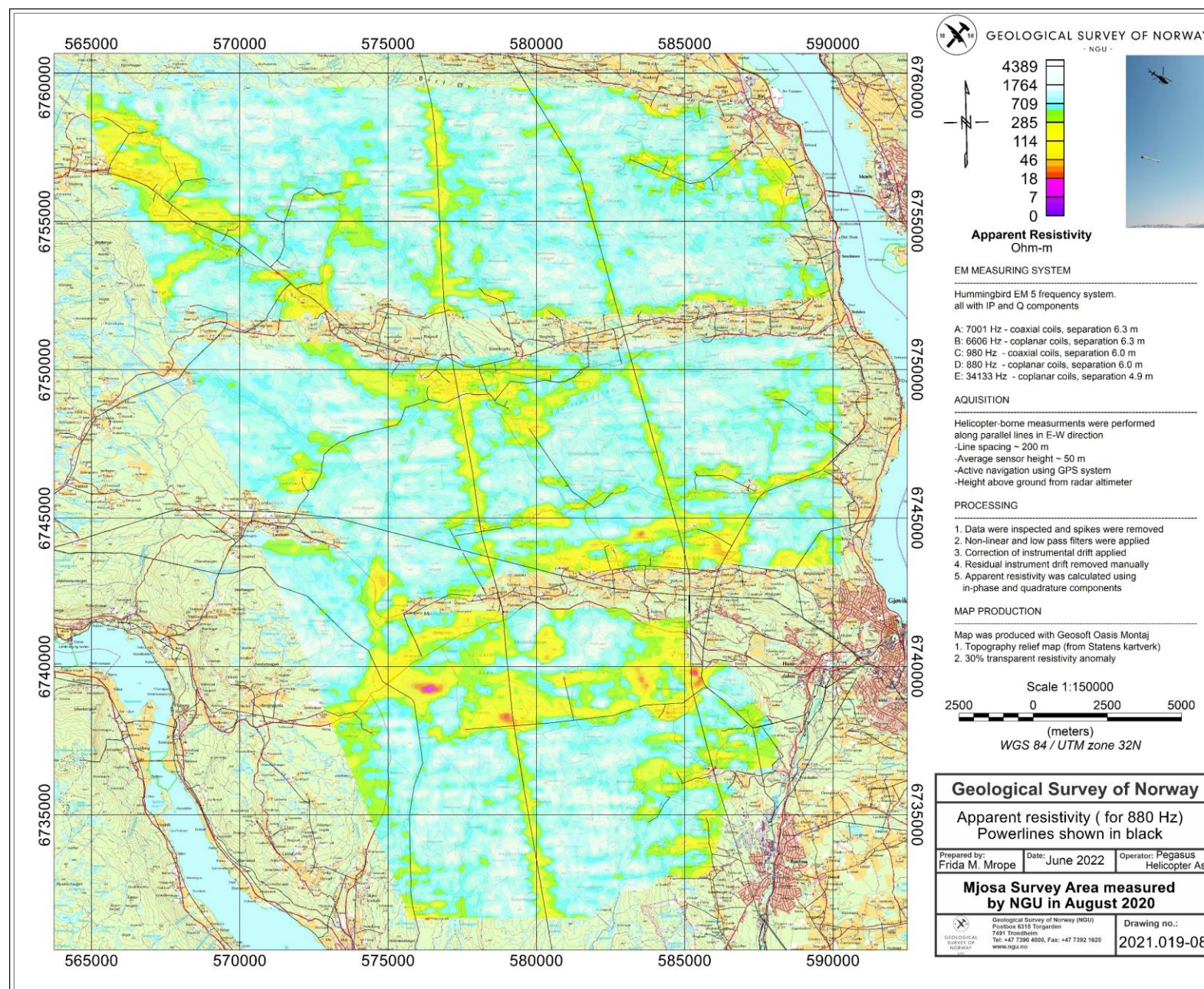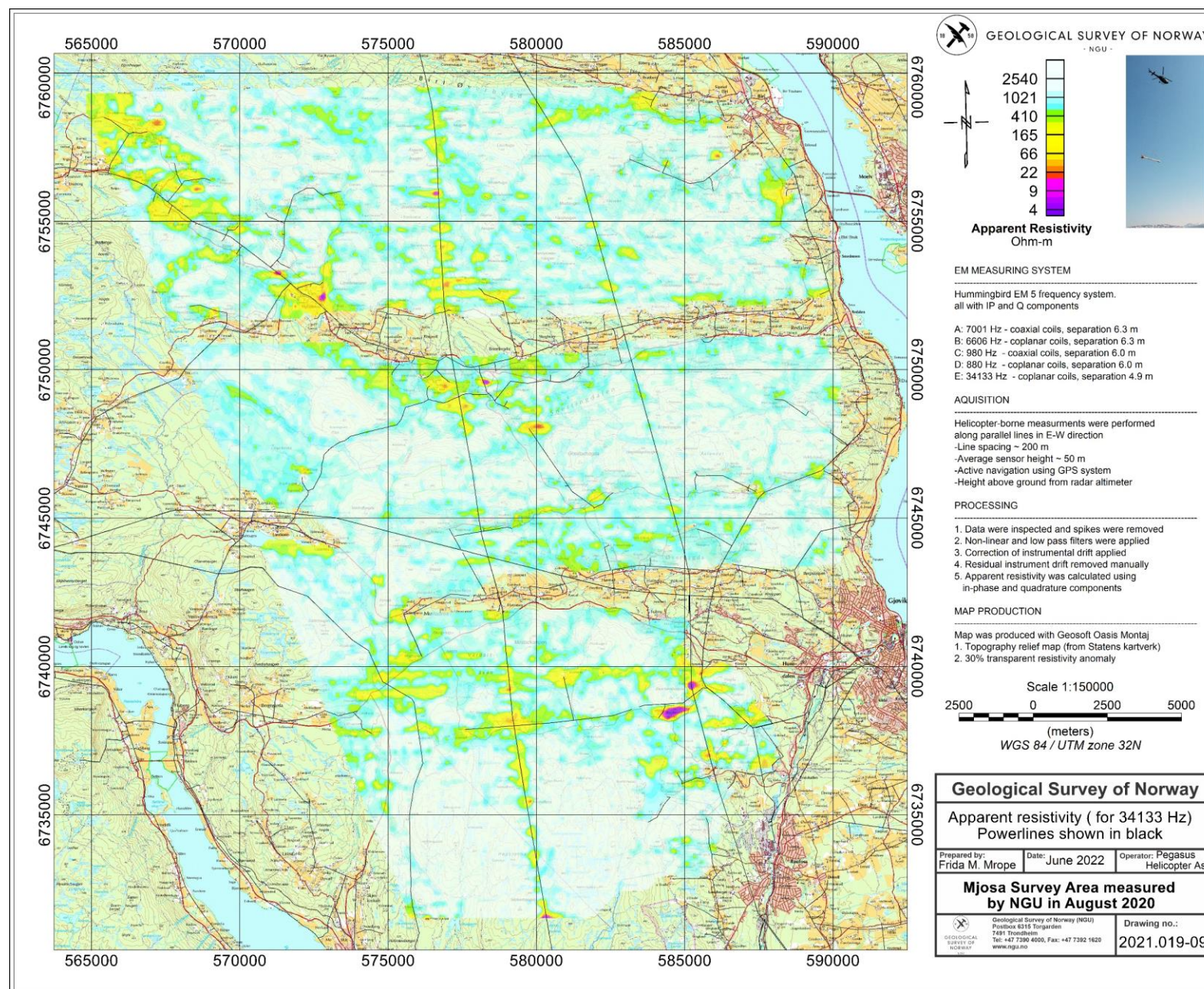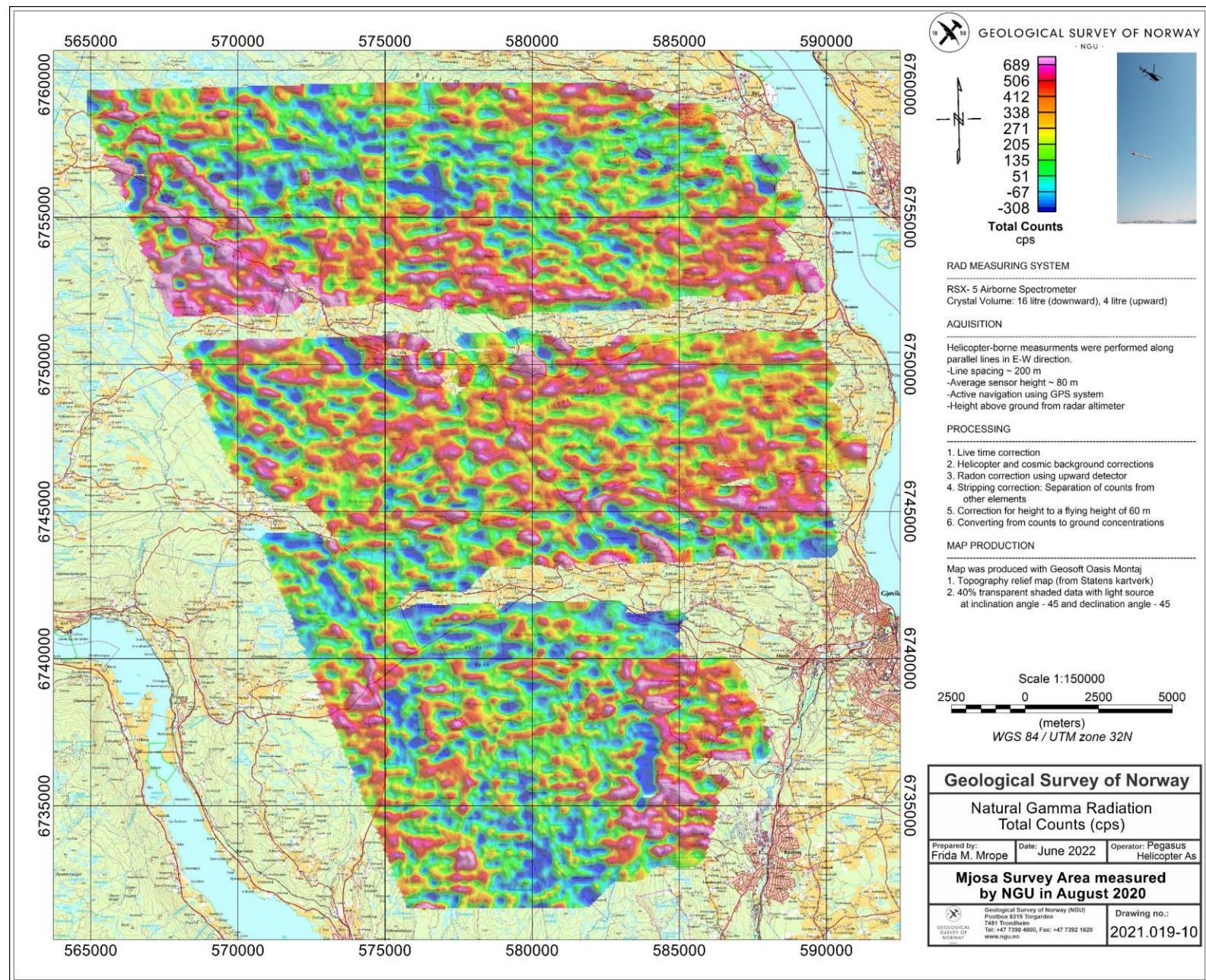**Figure 11: Apparent resistivity. Frequency 980 Hz, Coaxial coils.**

Figure 12: Apparent resistivity. Frequency 880 Hz, Coplanar coils.

Figure 13 Apparent resistivity. Frequency 34133 Hz, Coplanar coils.

Figure 14: Radiometric Total counts.
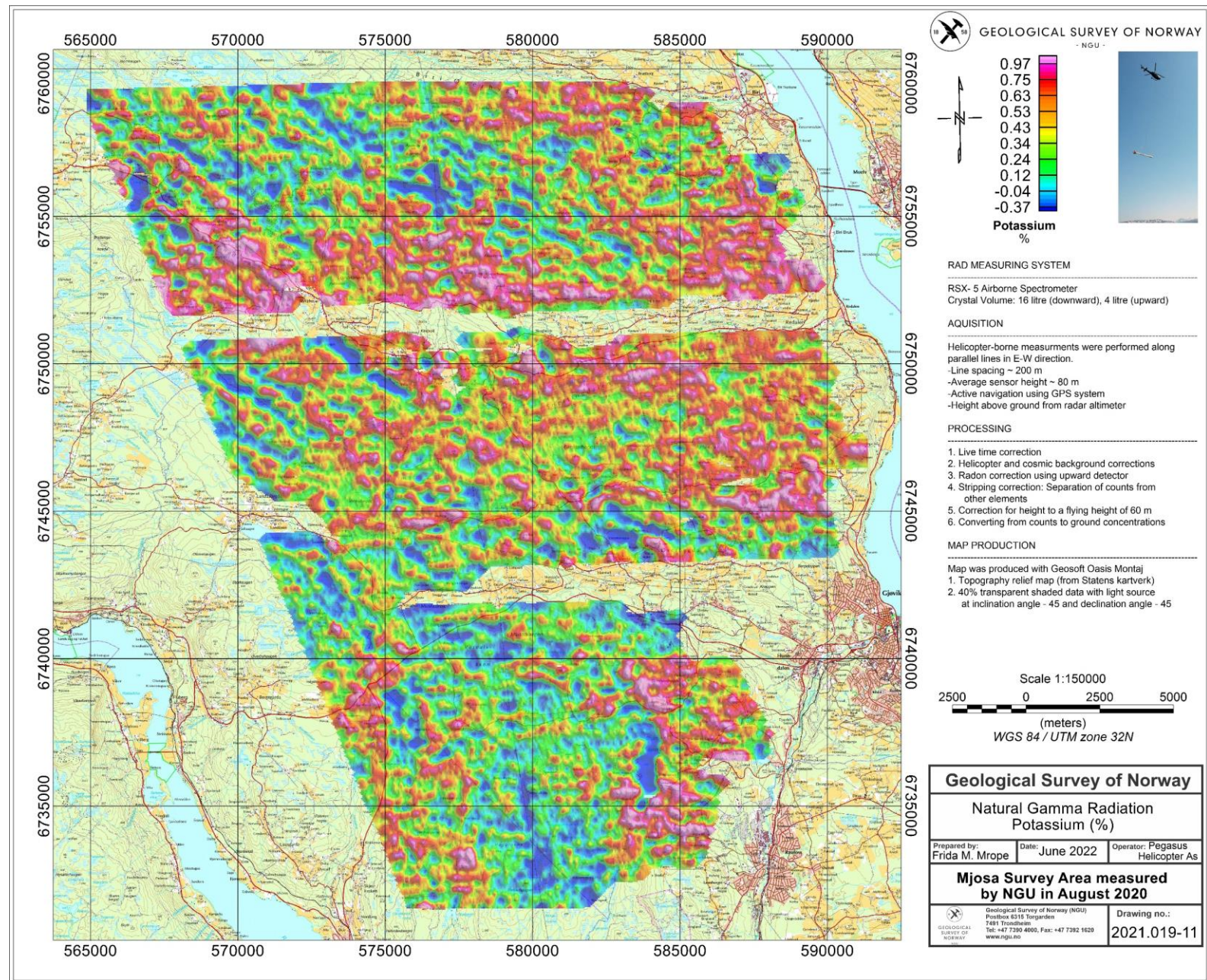
Figure 15: Potassium ground concentration.
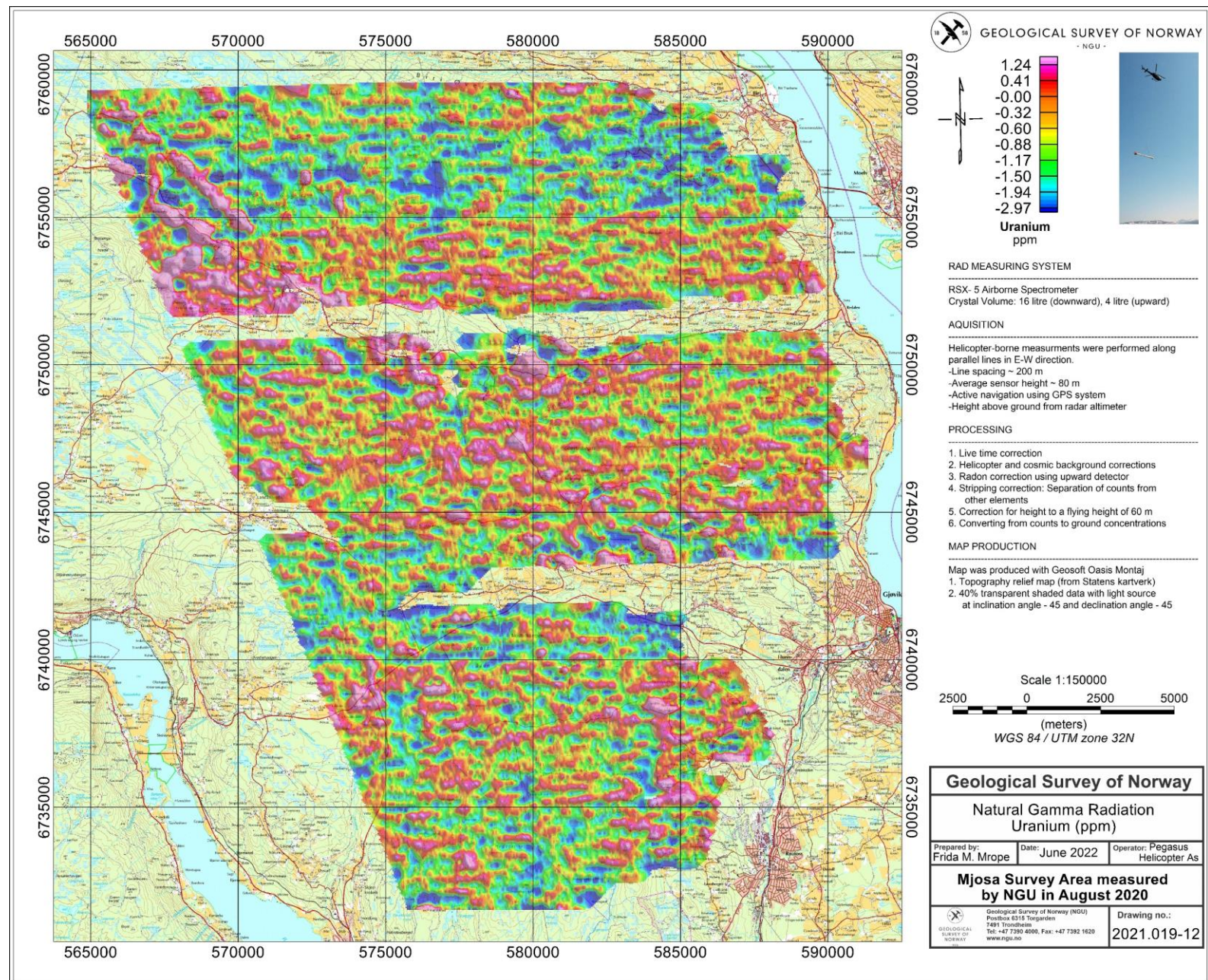
Figure 16: Uranium ground concentration.
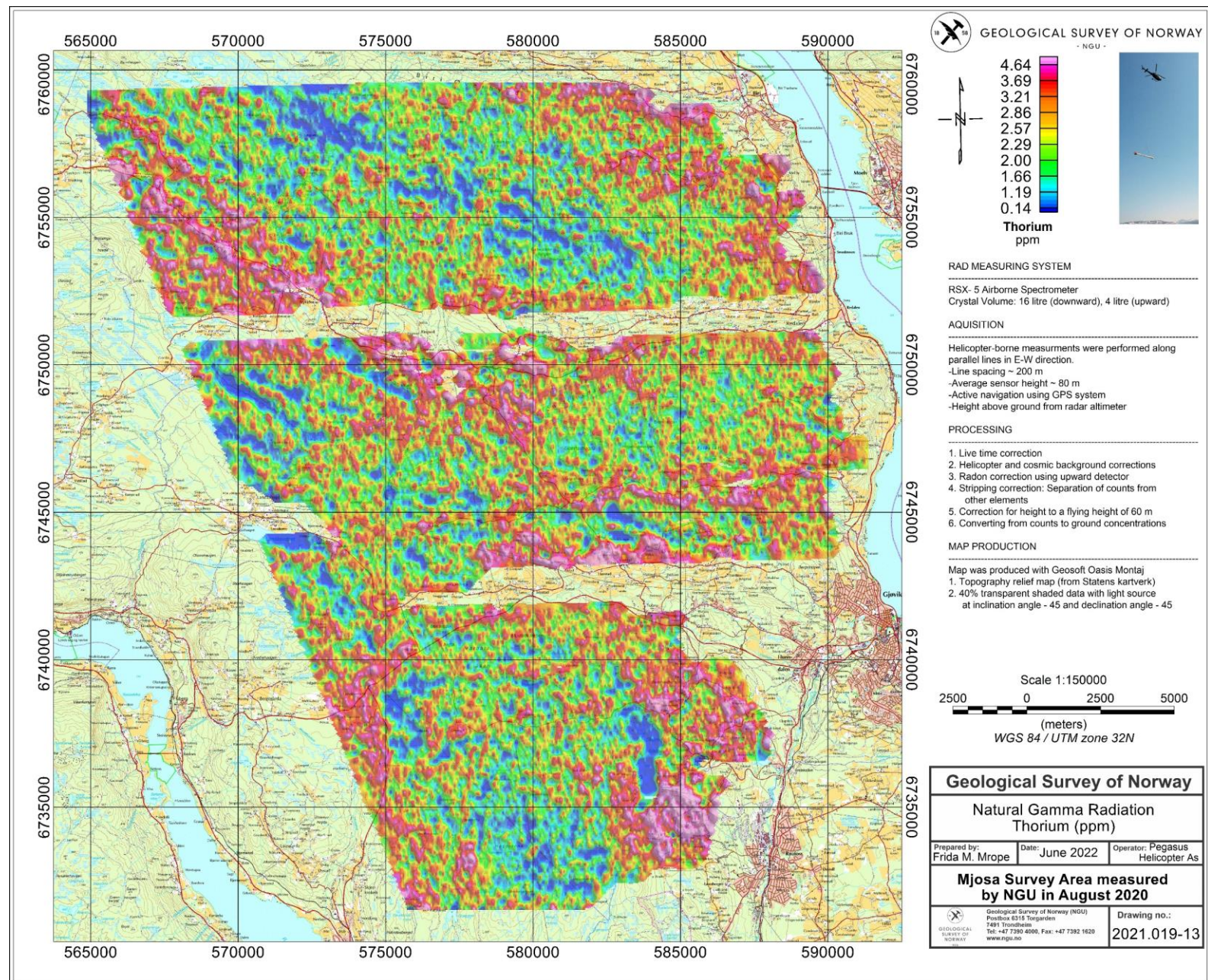
Figure 17: Thorium ground concentration.

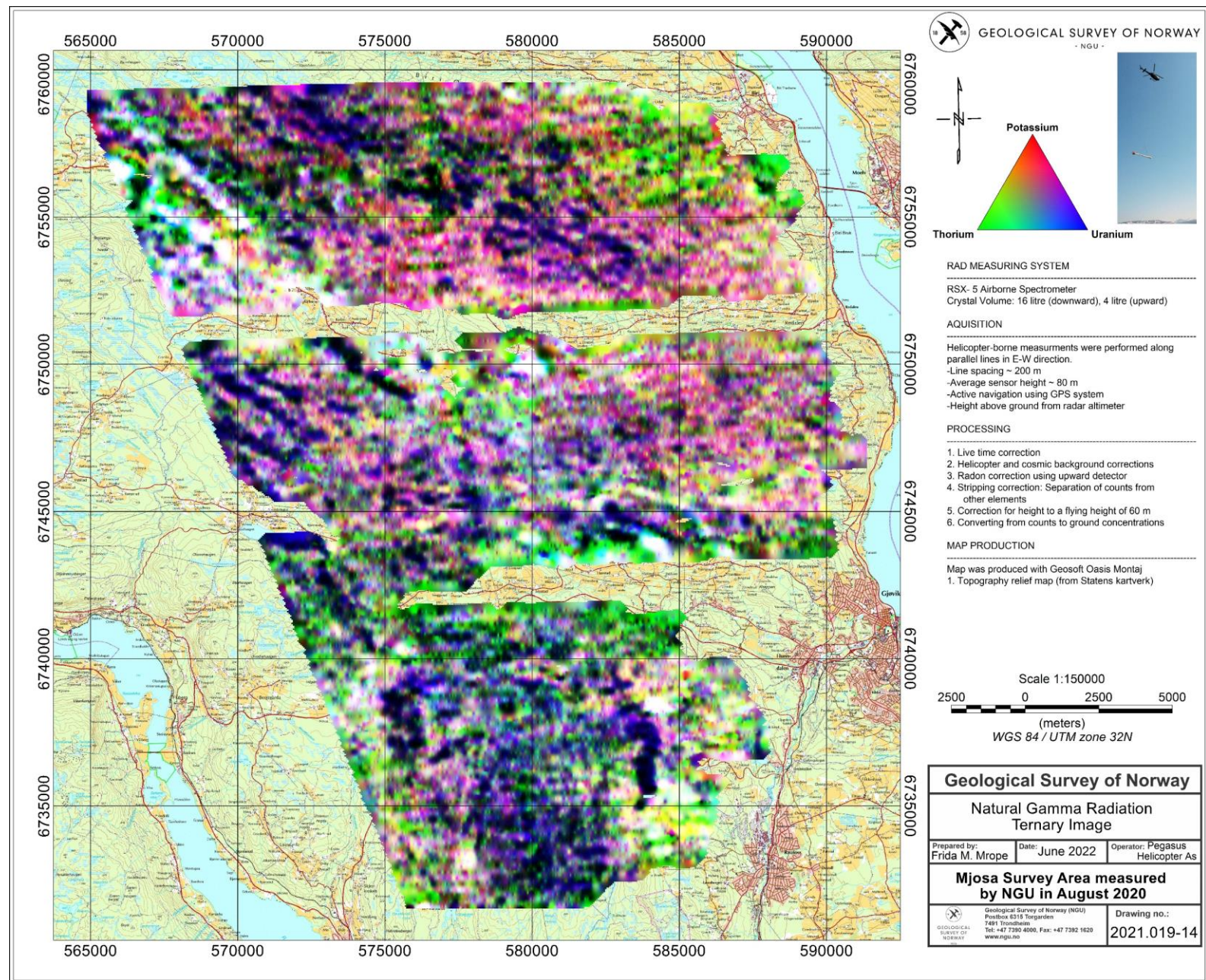**Figure 18: Radiometric Ternary Image.**

35